JOURNAL OF APPLIED ELECTROCHEMISTRY 24 (1994) 858–862

Further studies of a zinc–air cell employing a packed bed anode
Part III: Improvements in cell design

J. C. SALAS-MORALES, J. W. EVANS*

Department of Materials Science and Mineral Engineering, University of California Berkeley CA 94720, and Lawrence Berkeley Laboratory

Received 8 November 1993; revised 15 January 1994

A laboratory-scale zinc–air cell described previously has been redesigned with the intention of improving its performance. The zinc was present as a packed bed of 600 μm particles and in this concept the electrolyte and particles are replaced with fresh ones at the end of discharge, permitting the use of a monofunctional air electrode. The improved design had a reduced electrolyte volume on the air side of the cell and better electrical connection to the bed of particles, along with more conveniently located conduits for electrolyte flow driven by natural convection. When discharged at room temperature under the Simplified Federal Urban Driving Schedule (SFUDS) regimen (modified to eliminate regenerative braking) the cell yielded energies that were 2.8 times higher than the original cell (Part I). Increasing the cell temperature (up to 55 °C) was found to bring further improvements. Natural convection was shown to be necessary for good cell performance.

1. Introduction

Part I [1] of this three-part paper described the results of discharge experiments on a zinc–air cell where the zinc was present in the form of a packed bed of particles. The principal features of the cell were that it was intended for 'mechanical' refueling rather than electrical recharging, thereby avoiding the need for a bifunctional air electrode, and that the necessary flow of electrolyte was achieved by natural convection thus avoiding pumping [2].

The cell was intended for electric vehicle applications but must be distinguished from other particulate zinc–air cells where the zinc is present as a slurry [3]. There is some similarity to the zinc–air cell of Luz Electric Fuel (now Electric Fuel) [4] in that both cells require regeneration of particles and electrolyte external to the battery, a topic treated in Part II [5].

The present paper describes modifications to the cell design and resulting improved cell performance. The results of additional experiments demonstrating the efficacy of the solutal natural convection, cell performance at 55 °C and the ageing of the air electrode are included.

2. Apparatus and procedure

The cell used in this investigation is depicted in Fig. 1. The bed of zinc particles is stationary and 5–6 mm thick; it is held between a copper current collector (1.5 mm thick) and a diaphragm (Celgard 5550). On each side of the bed a channel (3 mm × 6 mm) serves as an anolyte reservoir and conduit for electrolyte. Due to the anodic dissolution of zinc, the electrolyte between the particles becomes denser than that in the conduits, providing the convection necessary for mass transport to and from the particle surfaces. The design is seen to be different from the concept described in an earlier paper [1, 6] where the electrolyte return path was behind the current feeder. The present design facilitates the stacking of cells and, if required, a reduction of electrolyte volume within the cell.

The cathode, separated from the diaphragm by a gap of 5 mm, was an AE-20 air electrolyte from Electromedia Corporation, with a 77 cm^2 active area. Contact to the nickel mesh on the air electrode was made via a copper mesh protruding through the top of the cell. Filtered air was fed through wash bottles (concentrated potassium hydroxide and distilled water) to the air side of the cell. In all experiments the air electrode was wetted with potassium hydroxide solution for at least 12 h prior to discharge.

The cell was built from Plexiglass; 600 μm zinc particles (Fisher Scientific Corporation) and reagent-grade potassium hydroxide were used. In a typical experiment, zinc particles, previously soaked in KOH, were placed on to the current collector with the cell in the horizontal position, the cell was assembled and filled with electrolyte in the upright position.

The cell was discharged through a Keithley bipolar power supply (model 228A) operated under the control of a microcomputer. The same computer recorded cell current and voltage. In some experi-

* Author to whom correspondence should be addressed.

0021-891X

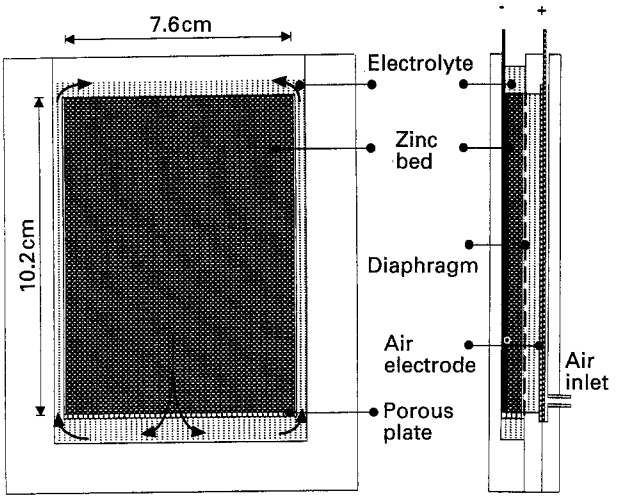

Fig. 1. Schematic of the 77 cm^2 laboratory cell in cross section.

ments a Luggin capillary was placed next to the diaphragm and connected to a Hg/HgO reference electrode. Discharge experiments were conducted either at constant current or using a modified SFUDS (Simplified Federal Urban Driving Schedule) cycle. Modification consisted of eliminating the regenerative braking of the SFUDS cycle (the current then being zero during these intervals) because the AE-20 electrode is degraded rapidly by reversal of current. Each 360 s cycle consisted of one peak of 8.06 W and three secondary peaks of 1.02, 2.05 and 5.10 W. Discharge was terminated when a preset minimum voltage was reached at the 8.06 W peak.

No temperature control was provided in room-temperature experiments but preliminary measurements indicated that the cell temperature remained between 298 K and 301 K. For higher-temperature runs the cell was immersed in a constant-temperature bath.

3. Results and discussion

3.1. *Room-temperature SFUDS discharge*

Figure 2 shows results from an SFUDS discharge experiment; cell voltage at room temperature at the SFUDS peak of 8.06 W is plotted versus extent of discharge to the point where the voltage reached 0.8 V at 16 Ah. This should be contrasted with charges of 7 to

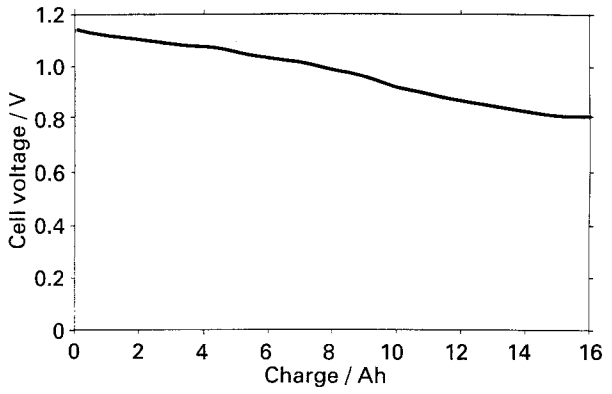

Fig. 2. Cell voltage at peak power for a SFUDS discharge.

Table 1. Comparative projections for a 55 kW battery

	Savaskan et al. [*1*]	*This model*
Cut-off voltage per cell (V)	0.8	0.8
SFUDS peak power (kW)	55	55
SFUDS energy (kWh)	62	127
SFUDS specific power ($W kg^{-1}$)	97	88
SFUDS specific energy ($Wh kg^{-1}$)	119	202

8 Ah observed under similar conditions in the previous investigation [1]. The improvement is ascribed to the improved current feeder and the way in which electrical connections were made to the feeder.

Savaskan *et al.* [1] projected full-scale battery performance from laboratory results by assuming that the same power and energy per unit area of electrode would be achieved on the two scales. Furthermore it was assumed that the same zinc/electrolyte ratio would apply and allowance was made for the weight of the battery construction materials and the air scrubbing system. Results of that projection appear in Table 1 along with projections based on the performance of the present cell.

Figure 3 shows the electrolyte potentials versus a Hg/HgO electrode for the start and end of the discharge of Fig. 2. Taking the conductivity of the electrolyte-saturated diaphragm to be 0.103 $S cm^{-1}$ [7] and the electrolyte conductivities to be 0.5 $S cm^{-1}$ and 0.4 $S cm^{-1}$ [8] for the start and end of discharge, respectively, the results of Fig. 3 permit an estimate of potential distribution in the cell. This estimate is shown schematically in Fig. 4, where the potential shown in the bed is that of the electrolyte. The reduction in cell voltage during discharge is therefore attributed to (a) a polarization of the zinc bed, due to reduction of the conductivity of the electrolyte, coupled with variation in the distribution of reaction in the bed (see below) and (b) polarization of the air electrode. The electrolyte on the air side of the cell sustains a potential drop of approximately 80 mV. Because this electrolyte plays little role in maintaining zinc species in solution it was conjectured that the 5 mm separation between diaphragm and air electrode could be reduced with consequent improvement in specific power and energy. This conjecture is examined below (Section 3.2).

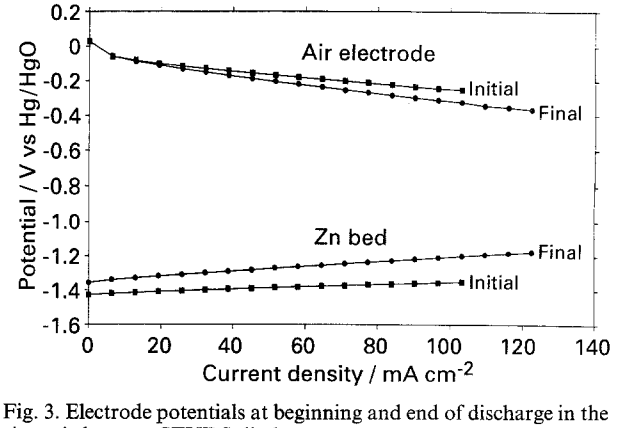

Fig. 3. Electrode potentials at beginning and end of discharge in the zinc–air battery, SFUDS discharge.

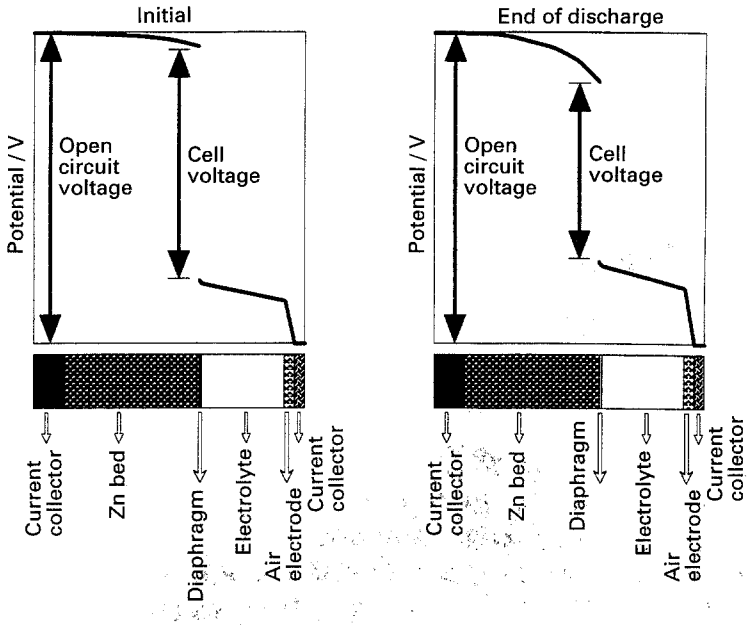

Fig. 4. Semi-empirical schematic distribution of potentials in the zinc–air battery, SFUDS discharge.

Replacement of the anolyte at the end of discharge resulted in some recovery of the cell voltage from its value at the end of discharge, but a second discharge led to the cut-off voltage (0.8 V) being reached at half the charge passed of the first discharge [9]. These results indicate that, even when the conductivity of the electrolyte plays an important role, the cell potential is also affected by changes occurring in the zinc bed. These could be the diminution of the zinc surface area or precipitation of zinc oxide on to the bed (although no precipitation was seen in the electrolyte in these experiments).

Figure 5 shows the polarization curves for the zinc bed following 2 Ah discharges under the normal SFUDS cycle and a higher power SFUDS cycle (1.25 SFUDS, i.e., peak = 8.06 W × 1.25 = 10.1 W). It is seen that the polarization curve is dependent not just on the state of charge but on how that state is reached.

3.2. *Operation of cell with reduced electrolyte volume*

The air side of the cell was redesigned to place the air electrode directly against the diaphragm; reducing total electrolyte volume from 70 cm^3 to 21 cm^3. The improved performance on discharge is evident in a comparison (Table 2) between this modification and the cell used to generate the results of Fig. 2. Applying the scale-up algorithm described above (Section 3.1) permits these results to be projected to a 55 kW battery (Table 3). The redesigned cell appears to be a significant improvement.

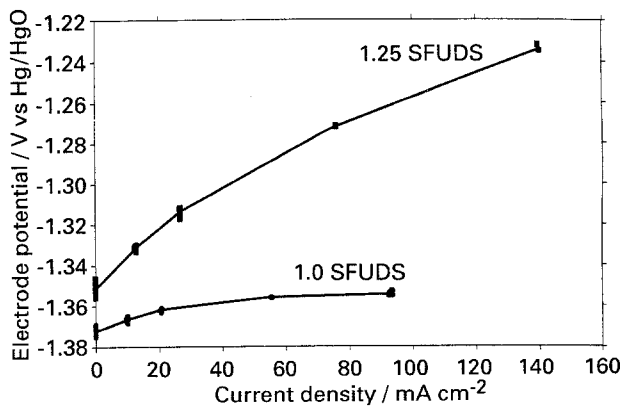

Fig. 5. Polarization curves of the zinc bed for two different paths of discharge. Total charge withdrawn 2 Ah.

3.3. *The significance of the anolyte recirculation channels*

As shown in Fig. 1, channels are provided alongside the bed to promote natural convection. However, the electrolyte within the channels contributes to the mass of the cell, suggesting that the specific power might be improved by their elimination. An experiment was conducted to determine the effect of the natural convection. To distinguish this effect from one due to electrolyte volume, that volume was kept constant; the channels were closed with small quantities of Hypalon sealant. The effects are shown in Table 4 and Fig. 6. It appears that the channels are effective in enhancing the performance of the cell. In a separate investigation [10] electrolyte velocities within the channels have been measured by the laser-Doppler velocimetry and will be reported subsequently.

3.4. *Effect of cell temperature*

Figure 7 displays the effect of cell temperature on electrolyte polarization prior to discharge. The effect is small for the zinc electrode but significant for the air

Table 2. Performance of a cell with reduced electrolyte volume

	Previous cell	*Reduced volume*
Temperature	room	room
Electrolyte volume (cm^3)	70	21
SFUDS peak power (W)	8.06	8.06
SFUDS charge (Ah)	15.9	17.3
SFUDS energy (Wh)	18.6	20.3

Table 3. Scaled-up performance for a 55 kW battery with reduced electrolyte volume

Total mass (kg)	417
SFUDS peak power (kW)	55
SFUDS energy (kWh)	139
SFUDS specific power ($W kg^{-1}$)	132
SFUDS specific energy ($Wh kg^{-1}$)	333

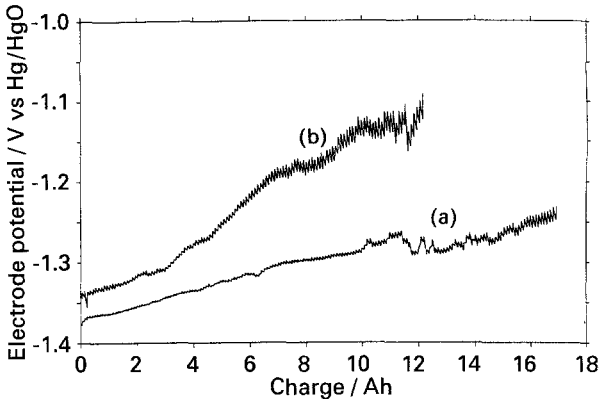

Fig. 6. Comparison of electrode potentials at peak power (8 W) for SFUDS discharge in cell (a) with and (b) without recirculation channels.

electrode; as expected, the kinetics of oxygen reduction are enhanced at the higher temperature.

One run was carried out in the range 55–60 °C, using the cell at reduced electrolyte volume (Section 3.2). The run was intended to simulate discharge of a battery at high power and the normal SFUDS peaks were multiplied by 1.9. Table 5 shows the results of this discharge and scale-up to a 55 kW battery.

3.5. *Aging of the AE-20 air electrode*

Electrode polarization curves for a new air electrode placed in the cell and after 250 SFUDS cycles at 55 °C appear in Fig. 8. There appears to be a significant deterioration of the air electrode.

4. Possibilities for further improvement

The electrolyte within the zinc–air cell described here is approximately one quarter of the battery weight.

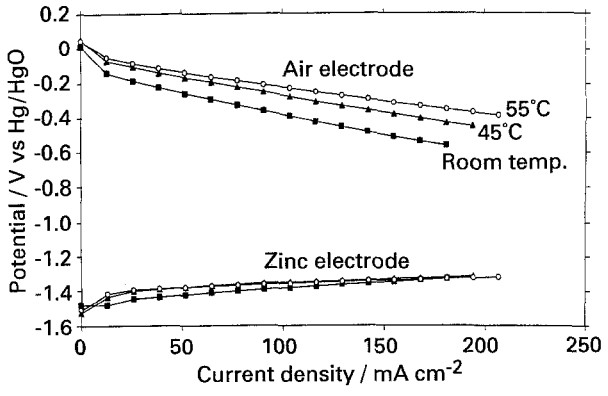

Fig. 7. Effect of temperature on electrode potentials. Undischarged cell.

Table 4. Effect of anolyte recirculation channels

	Open channels	*Closed channels*
Temperature (°C)	room	room
Electrolyte volume (cm^3)	21	21
SFUDS peak power (W)	8.06	8.06
Charge (Ah)	17.3	12.2
Energy (Wh)	20.3	14.0

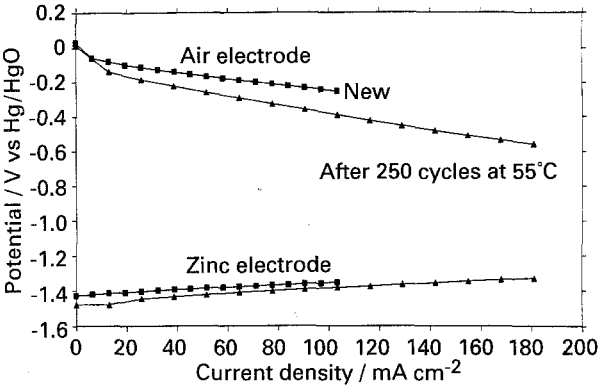

Fig. 8. Aging of the AE20 air electrode.

The thesis [9] on which this paper is based discusses the possibility of reducing the electrolyte mass by reducing the KOH concentration.

Alternatively, the second most massive part of the battery is the zinc and Fig. 4 indicates that a substantial drop in potential occurs across the bed of particles, particularly towards the end of discharge. These suggest that the performance might be further improved by a reduction of bed thickness. This possibility was examined by using the well known porous electrode model [11–13] with parameters appropriate for the electrochemistry of this cell [9].

Figure 9 shows the computed potential for two electrolyte conductivities corresponding to the start ($0.45 S cm^{-1}$) electrolyte and end ($0.19 S cm^{-1}$) electrolyte. The profiles are for a 6.5 mm bed. It is seen that one half or less of the bed is electrochemically active. It is estimated that bed thicknesses less than 4 mm are precluded by the need to evacuate and replenish the particles. Consequently the model

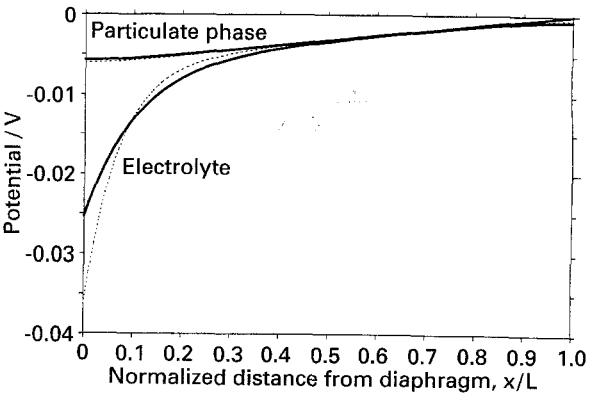

Fig. 9. Potential profiles for a zinc packed bed in KOH. $L = 0.65 cm$, $\sigma_p = 5 S cm^{-1}$, $i_0 = 0.03 A cm^{-2}$, $a = 30 cm^{-1}$, $I = 0.050 A cm^{-2}$, current collector at $x = L$. Curves: (——) $\sigma_e = 0.45 S cm^{-1}$ and (· · · · ·) $\sigma_e = 0.19 S cm^{-1}$.

Table 5. Performance at 55–60 °C high power discharge

(a) Bench scale results	
Volume of electrolyte (cm^3)	21
SFUDS peak power (W)	15.0
Charge (Ah)	5.0
Energy (Wh)	5.2
(b) Scale up to 55 kW	
Weight (kg)	189
SFUDS energy (kWh)	19
SFUDS peak power (kW)	55
SFUDS specific power ($Wh\,kg^{-1}$)	100
SFUDS specific power ($W\,kg^{-1}$)	290

calculations were repeated for a 4 mm thick bed; the results [9] show that reaction is now distributed throughout the bed although it is still skewed towards the diaphragm. A minor improvement in cell voltage is predicted. At 4 mm the reduction in weight of components results in a reduction in battery weight and a corresponding increase in specific power is anticipated.

5. Concluding remarks

Estimated battery performance based on the laboratory experiments described in this paper are summarized in the Ragone plot of Fig. 10. The values are for modified SFUDS discharge. Improvements have been achieved by modifications such as the elimination of electrolyte in the cathodic side of the cell and redesign of the anodic current feeder.

The decay in cell voltage observed during discharge occurs because of changes in both electrodes. Cell voltages are higher at higher temperatures primarily due to higher air electrode potentials although at the highest temperatures there may be degradation of the air electrode used here.

The need for conduits through which natural convection can occur has been demonstrated. In the improved cell these conduits are of reduced volume and arranged alongside the bed so as to facilitate stacking of cells.

The cell appears to offer the prospect of being suitable for its intended application, i.e. in meeting the near-term goals and approaching the long-term goals of the US Advanced Battery Consortium.

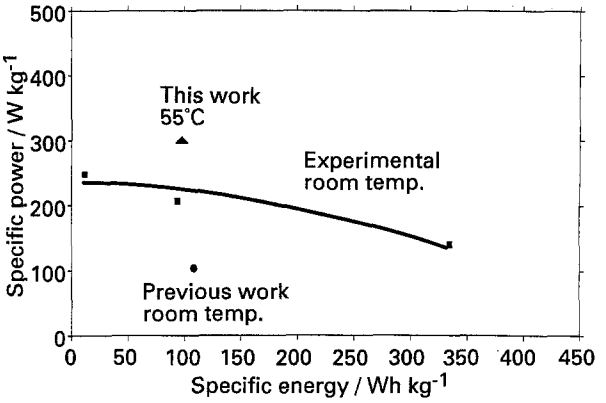

Fig. 10. Ragone plot for the Zn–air battery with natural convection.

Acknowledgement

This work was supported by the Assistant Secretary for Energy Efficiency and Renewable Energy, Office of Transportation Technologies, Electric and Hybrid Propulsion Division of the US Department of Energy under contract DE-AC03-76SF00098.

References

[1] G. Savaskan, T. Huh and J. W. Evans, *J. Appl. Electrochem.* **22** (1992) 909.
[2] G. Savaskan and J. W. Evans, 'Battery Using a Metal Particle Bed Electrode', *US Patent 5 006 424*, Apr. (1991).
[3] A. J. Appleby, J. P. Pompon and M. Jacquier, Proceedings of the 10th Intersociety Energy Conversion Engineering Conference. IECEC '75, Newark, Delaware (1975), pp. 811–816.
[4] B. Koretz, J. Goldstein, Y. Horats and M. Korall, paper presented to the 25th symposium on *Automotive technology and automation*, Florence, Italy, 2–5 June (1992).
[5] T. Huh, G. Savaskan and J. W. Evans, *J. Appl. Electrochem.* **22** (1992) 916.
[6] J. W. Evans and G. Savaskan, *ibid.* **21** (1991) 105.
[7] Celgard 5550 Data Sheet, Hoechst Celanese Corp., Nov. (1988).
[8] M. Liu, B. R. Faulds, G. M. Cook and N. P. Yao, *J. Electrochem. Soc.* **128** (1981) 2049.
[9] J. C. Salas-Morales, MS thesis, University of California, Berkeley, CA (1993).
[10] S. Siu, Ph.D dissertation, University of California, Berkeley, CA (1994).
[11] J. S. Newman and W. Tiedemann, *AIChE J.* **21** (1975) 25.
[12] J. S. Newman, Electrochemical Systems, 2nd edn, Prentice Hall, Englewood Cliffs, NJ (1991), pp. 454–495.
[13] Z. Mao and R. E. White, *J. Electrochem. Soc.* **139** (1992) 1105.